FORMATION AND TRANSFORMATION OF ANTIFERROMAGNETIC DOMAINS IN METALLIC MULTILAYERS: THE REFLECTOMETRIC APPROACH

D.L. NAGY, L. BOTTYÁN, L. DEÁK, M. MAJOR and E. SZILÁGYI

KFKI Research Institute for Particle and Nuclear Physics, Budapest, Hungary, nagy@rmki.kfki.hu

ABSTRACT

The magnetocrystalline anisotropy in antiferromagnetically (AF) coupled metallic multilayers may lead to spectacular effects, which can be most efficiently studied by two closely related nuclear scattering techniques, namely synchrotron Mössbauer reflectometry (SMR) and polarised neutron reflectometry (PNR). A spin-flop transition takes place in a strongly AF-coupled epitaxial Fe/Cr multilayer of fourfold in-plane anisotropy when a moderate magnetic field is applied along the easy axis in which the layer magnetisations actually lay. The electronically forbidden AF reflections in a specular SMR experiment fully appear or completely disappear during the spin-flop transition. In case of specular PNR, the AF reflection moves from the spin-flip to the non-spin-flip channel on spin-flop transition or vice versa. The off-specular SMR and PNR techniques are sensitive to the in-plane correlation length ξ of the layer magnetisation direction and are, thereby, able to map the size distribution of the AF domains in multilayers. A dramatic increase of ξ from about 1 μm to at least 10 μm, i.e., a coarsening of the AF domains was observed in the same multilayer when it passed the spin-flop transition provided that the external magnetic field was previously decreased from magnetic saturation to zero. This shows the key role of the in-plane magnetocrystalline anisotropy in the domain-coarsening process. Finally we demonstrate how the formation of sub-micrometer domains can be followed by SMR and PNR.

Keywords: Multilayers, antiferromagnetic coupling, domains, synchrotron Mössbauer reflectometry, polarised neutron reflectometry

1. Introduction

Total external reflection (TER) of x-rays [1] and neutrons [2] from flat surfaces are phenomena dating back to the first half of the twentieth century. The real part of the index of refraction n of most materials for thermal neutrons and of all materials for non-resonant x-rays is by about 10^{-5} less than unity. At low enough angles of grazing incidence $\Theta < \Theta_c = \sqrt{2(1-n)}$ the waves are totally reflected. The intensity of the reflected specular beam for $\Theta > \Theta_c$ rapidly decreases with increasing wave vector transfer (scattering vector) $q = 2k \sin\Theta$ where k is the length of the wave vector of the incident radiation. In a stratified medium, reflected and refracted beams appear at each interface. The interference of the reflected beams leads to patterns of the reflectivity vs. scattering vector spectrum $R(q)$ that bear information on the depth profile of the index of refraction $n(z)$, the argument z being the co-ordinate per-

pendicular to the sample surface. $R(q)$ can be calculated from $n(z)$, e.g., using the method of *characteristic matrices* [3]. Therefore, in frames of a given model for the stratified system, $n(z)$ can be reconstructed (the parameters of the model can be fitted) from $R(q) = |r(q)|^2$ where $r(q)$ is the reflectivity amplitude. This latter approach is the basic idea of specular *x-ray* and *neutron reflectometry*, two methods that can be used for mapping the electron density and the isotopic/magnetic structure of thin films, respectively.

In fact, the coherent forward scattering of a scalar wave of momentum much higher than that of the scattering centres can be described [4] by the index of refraction close to unity

$$n = 1 + \frac{2\pi N}{k^2} f \tag{1}$$

where N is the density of the scattering centres and f is the scattering amplitude. The electron density for non-resonant x-rays or nuclear and magnetic scattering length density for neutrons is included in the latter quantity.

X-ray reflectometry may optionally be performed with resonant photons. One approach, which we will not discuss here, is the grazing-incidence resonant x-ray scattering (RXS), i.e., x-ray reflectometry performed at absorption edges. At suitable absorption edges, due to the circular dichroic effect, RXS becomes sensitive to the magnetisation, a reason for alternatively referring to this technique [5] as 'x-ray magnetic resonant scattering'. A drawback of grazing-incidence RXS is the fact that, in case of 3d transition metals, a considerable magnetic effect can only be observed at the L absorption edges, which have an energy < 1 keV. Since the penetration depth of soft x-rays at grazing incidence hardly exceeds a few nanometers, the possible application of grazing-incidence RXS for studying the magnetic structure in thin films of 3d transition metals remains quite limited.

The other approach is to use nuclear resonant photons, i.e., photons capable of exciting a Mössbauer transition. We shall call this technique, henceforth, *Mössbauer reflectometry* (MR). MR benefits from the fact that, close to the nuclear resonance, the photon scattering amplitude f is strongly energy-dependent and contains the matrix elements of the hyperfine interactions. MR is, therefore, suitable to study the magnetic structure of thin films. Since the typical Mössbauer transition energies lye in or even above the hard x-ray region, due to their higher penetration depth, MR is well suited to study the magnetic structure of deeper-lying layers in thin films.

A serious limitation of MR with conventional sources [6] is the small ($\sim 10^{-5}$) solid angle involved. Due to its high collimation, synchrotron radiation (SR) is much better suited for reflectometric experiments than radioactive sources. *Synchrotron Mössbauer reflectometry* (SMR) is the application of grazing-incidence nuclear resonant scattering of SR [7] to thin film and multilayer structure analysis. An important step towards the realisation of SMR was the observation [8] of the *total reflection peak* [8,9], i.e., the high number of *delayed* photons appearing close to the critical angle of the *electronic* TER. This peak is formally identified with the zeroth-order Bragg peak in nuclear resonant specular reflection. Since the pioneering work by Toellner et al. [10], the last half decade saw an increasing number of SMR experiments including a recent extension of the technique to off-specular (diffuse) scattering [11]. SMR and its application to thin film magnetism have recently been reviewed in various papers [12–18]. The present paper is a modified and partly extended version of Refs. 15 and 16. We will show that, using SMR, it is possible to study the orientation of the layer magnetisation, spin-flop phenomena and magnetic domain structure.

SMR shows many similarities to a well-established method, namely polarised neutron reflectometry (PNR). SMR and PNR can be mapped onto each other and a common optical formalism of both techniques exists [19]. In view of excellent reviews on PNR [20,21], we will not describe this method here.

Akin to SMR, PNR is also sensitive to the direction of the layer magnetisation. This sensitivity is achieved by analysing the spin of the reflected neutrons. In case of a parallel orientation of the layer magnetisation and the neutron spin, the spin of the reflected neutrons is retained by magnetic scattering ('non-spin-flip scattering'). The perpendicular orientation of the layer magnetisation and the neutron spin contributes to events of spin-reversal ('spin-flip scattering').

2. Specular and off-specular SMR

A sketch of the experimental arrangement of an SMR experiment is shown in Fig. 1. The photons from the high-resolution monochromator hit the sample mounted on a two-circle goniometer of adjustable height at an angle of grazing incidence ω. Further slits and optional focusing elements (not shown in the figure) are installed both upstream and downstream the monochromator. The reflected (scattered) photons are detected by an avalanche photo diode (APD) the aperture of which may be limited by a slit in front of the detector. The adjustable detector height defines the scattering angle 2 Θ.

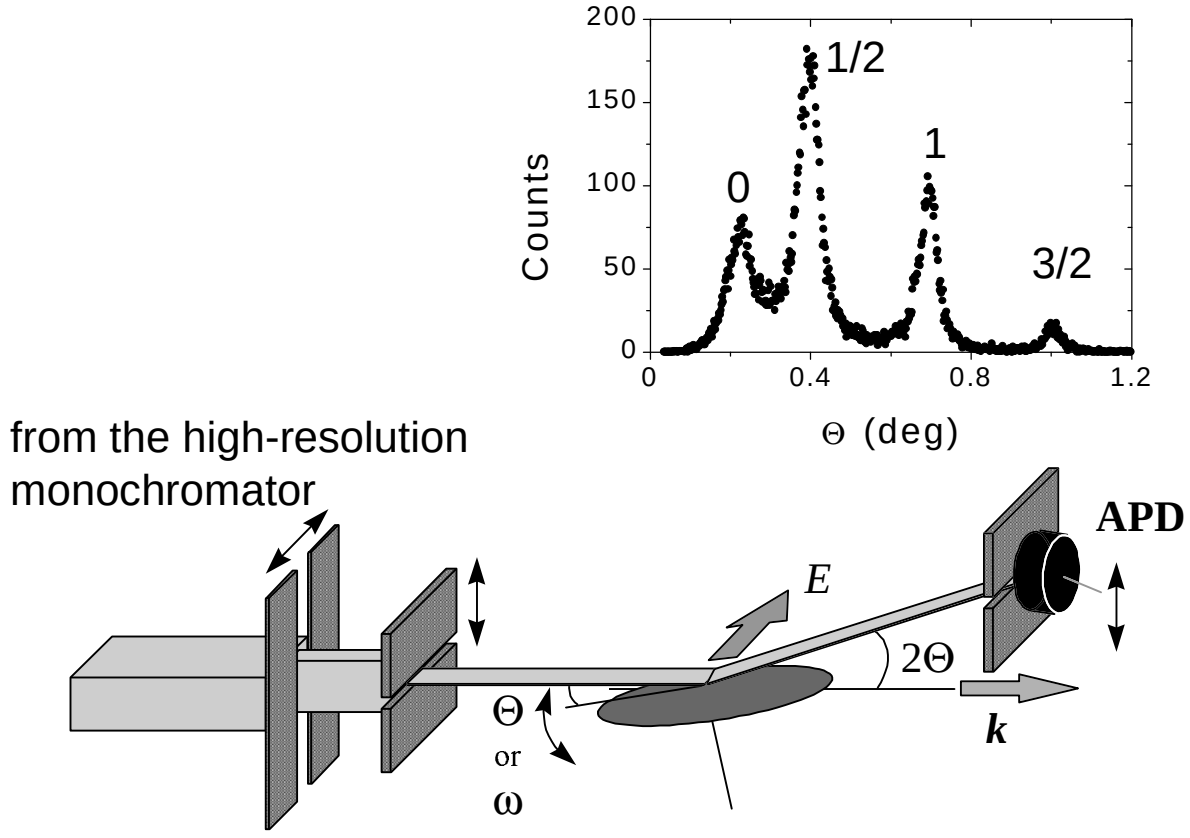

Fig. 1. *Experimental setup of an SMR experiment. The inset shows a Θ – 2 Θ scan measured at room temperature on a MgO(001)/[^{57}Fe(26Å)/Cr(13Å)]$_{20}$ multilayer with layer magnetisation parallel to the photon beam. The order of reflections is indicated, the half-order reflections being the antiferromagnetic peaks of pure nuclear origin.*

An SMR measurement is performed in either time-integral or time-differential regime. Time-integral SMR (TISMR) records the total number of delayed photons from t_1 to t_2 as a function of ω and/or Θ. Here t_1 is a few nanoseconds determined by the bunch quality of the radiation source and by the dead time of the detector and the electronics, while t_2 is set to a value somewhat below the bunch repetition time of the storage ring. Time-differential (TD) SMR is a time-response measurement performed at various fixed values of ω and Θ. In this paper we will restrict ourselves to TISMR.

Position-sensitive detectors have recently been increasingly applied in x-ray and neutron reflectometry in order to map the scattered intensity in a single experiment on the whole (ω,Θ) plane. Although APD arrays are being tested at various synchrotron facilities, as yet, TISMR experiments have only been performed in two different single-parameter geometries, namely $\Theta - 2\Theta$ scan and ω scan. In a $\Theta - 2\Theta$ scan the sample orientation and the detector height are simultaneously changed meeting the condition of specular reflection, $\omega = \Theta$. In an ω-scan experiment, 2Θ is fixed and ω is varied. As a rule, a scan of the *prompt* photons (i.e., non-resonant x-ray reflectometry) is recorded along with a delayed TISMR scan.

In a $\Theta - 2\Theta$ experiment the scattering vector $\underline{q}$ is perpendicular to the sample surface. For a periodic multilayer, in the first Born approximation (kinematical theory), Bragg maxima appear at $q = \sqrt{(2\pi/d)^2 + q_c^2}$, where d is the structural or hyperfine (magnetic) period length perpendicular to the film plane and q_c is the critical scattering vector of the TER (typically about 0.5 nm^{-1}). Thus a $\Theta - 2\Theta$ scan reveals the plane-perpendicular structure with the provision that the film is homogeneous in its plane. Should this not be the case, the intensity of the specular reflection is reduced. Lateral dimensions of inhomogeneities such as structural and magnetic roughness, waviness, magnetic domains, etc., however, cannot be further studied in a $\Theta - 2\Theta$ experiment.

In an ω-scan experiment, the condition of specular reflection is not fulfilled for $\omega \neq \Theta$. Off-specular scattered intensity is only significant in case of lateral inhomogeneities. In fact, for the small values of ω and Θ in this experiment, the perpendicular-to-plane component of the scattering vector is constant ($q_z = 2k\Theta$) while varying ω, the in-plane parallel-to-beam (longitudinal) component of the scattering vector is scanned: $q_x = 2k\Theta(\omega - \Theta)$. In order to have significant intensity, the detector height is set to meet the q_z value of a Bragg peak. The width of the ω scan (i.e., q_x scan) is, in first Born approximation, inversely proportional to the lateral, longitudinal correlation length ξ of the quantity the perpendicular-to-plane periodicity of which the Bragg peak is related to:

$$\xi = \frac{2\pi}{\Delta q_x} = \frac{\pi}{k\Theta\Delta\omega} \qquad (2)$$

where Δq_x and $\Delta\omega$ are the peak widths of the q_x and ω scans, respectively. Therefore, setting 2Θ in an ω-scan experiment to an electronically forbidden pure nuclear reflection, the lateral correlation length of inhomogeneities of the hyperfine interaction (magnetic roughness, magnetic domains) can be determined.

3. Layer magnetisation direction in coupled multilayers

The direction of the layer magnetisation is an important issue in thin-film magnetism. Its dependence on the applied magnetic field and temperature yields information on interlayer coupling and magnetic anisotropy. SMR can be used to determine the layer magnetisation direction in thin films and multilayers.

Pure nuclear superstructure reflections of antiferromagnetic (AF) origin appear in TISMR experiments performed on AF-coupled multilayers provided that the layer magnetisations and, consequently, the hyperfine magnetic fields are not perpendicular to the photon propagation direction. Indeed, under this condition, the scattering amplitudes f for the two kinds of magnetic layers of mutually antiparallel orientation of the magnetisation differ from each other by a phase factor, which is not the case for the perpendicular orientation where the scattering amplitudes are equal. For directions of the layer magnetisation between beam-parallel and beam-perpendicular orientations in an AF-coupled multilayer, the relative intensity of the AF peak is reduced, giving, thereby, an excellent tool for studying the

process of magnetic saturation. TISMR was applied to follow the saturation process in Zerodur/[^{57}Fe(2.55 nm)/^{nat}FeSi(1.5 nm)]$_{10}$ multilayer [22] and in MgO(001)/[^{57}Fe(1.43 nm)/Cr(3.06 nm)]$_{16}$ superlattice [15]. However, since the AF peak is suppressed for any beam-perpendicular direction of the layer magnetisation, a TISMR experiment cannot distinguish between out-of-plane and in-plane beam-perpendicular components of the layer magnetisation.

In contrast to specular SMR, where the AF reflection appears only in case of layer magnetisation parallel to the photon propagation direction, an AF reflection is always present in a specular PNR experiment, provided that the multilayer is AF-ordered. However, a PNR AF reflection appears in the non-spin-flip or in the spin-flip channel, according to whether the layer magnetisation is oriented parallel or perpendicular to the neutron spin, respectively.

4. Spin-flop phenomena

An interesting model system in multilayer magnetism is a periodic AF-coupled Fe/Cr superlattice with even number of Fe layers. When the external magnetic field is aligned along the easy axis of the Fe layers parallel/antiparallel to the layer magnetisations, the anisotropy-stabilised configuration becomes energetically unfavourable at a certain critical in-plane field strength and a sudden magnetisation reorientation is expected in a finite multilayer stack [23] with *surface spin-flop* [24,25] or *bulk spin-flop* (BSF) [26] scenarios, in cases of uniaxial and fourfold in-plane anisotropy, respectively. These processes are associated with major jumps of the direction of one or more layer magnetisation, but as a rule, only with minute changes of the net magnetisation. It is, therefore, not easy to identify a spin-flop transition with methods of classical magnetism.

As shown in the previous section, SMR is a sensitive tool to determine the layer magnetisation directions in thin films and multilayers. Therefore SMR is especially suitable for studying spin-flop phenomena. We have recently reported on TISMR of the (bulk) spin-flop in an AF-coupled Fe/Cr superlattice with a fourfold in-plane anisotropy [27,28].

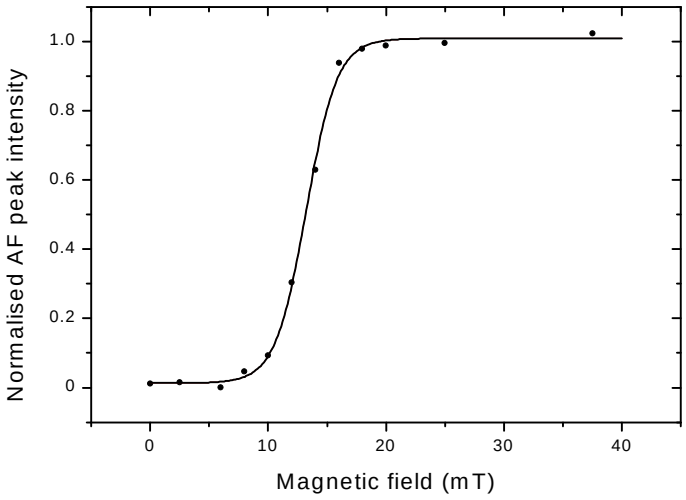

Fig. 2. *Normalised intensity of the AF peak of a MgO(001)/[^{57}Fe(26Å)/Cr(13Å)]$_{20}$ multilayer during bulk spin flop. The continuous line is guiding the eyes.*

The experiment at the nuclear resonance beamline ID18 of the European Synchrotron Radiation Facility was performed on a MgO(001)/[^{57}Fe(26Å)/Cr(13Å)]$_{20}$ multilayer [28] using the 14.413 keV resonance of ^{57}Fe. The epitaxial relationship on MgO(001) substrate is MgO(001)[110]//Fe(001)[100], therefore the magnetisation of the individual Fe layers points parallel or antiparallel to either of the Fe[010] or Fe[100] axes in the film plane. The initial magnetic state of the multilayer was carefully prepared by applying external magnetic field as described below. The scattering plane was vertical and the wave vector **k** of the incoming resonant beam was perpendicular to the in-plane magnetic field, as shown in Fig. 1.

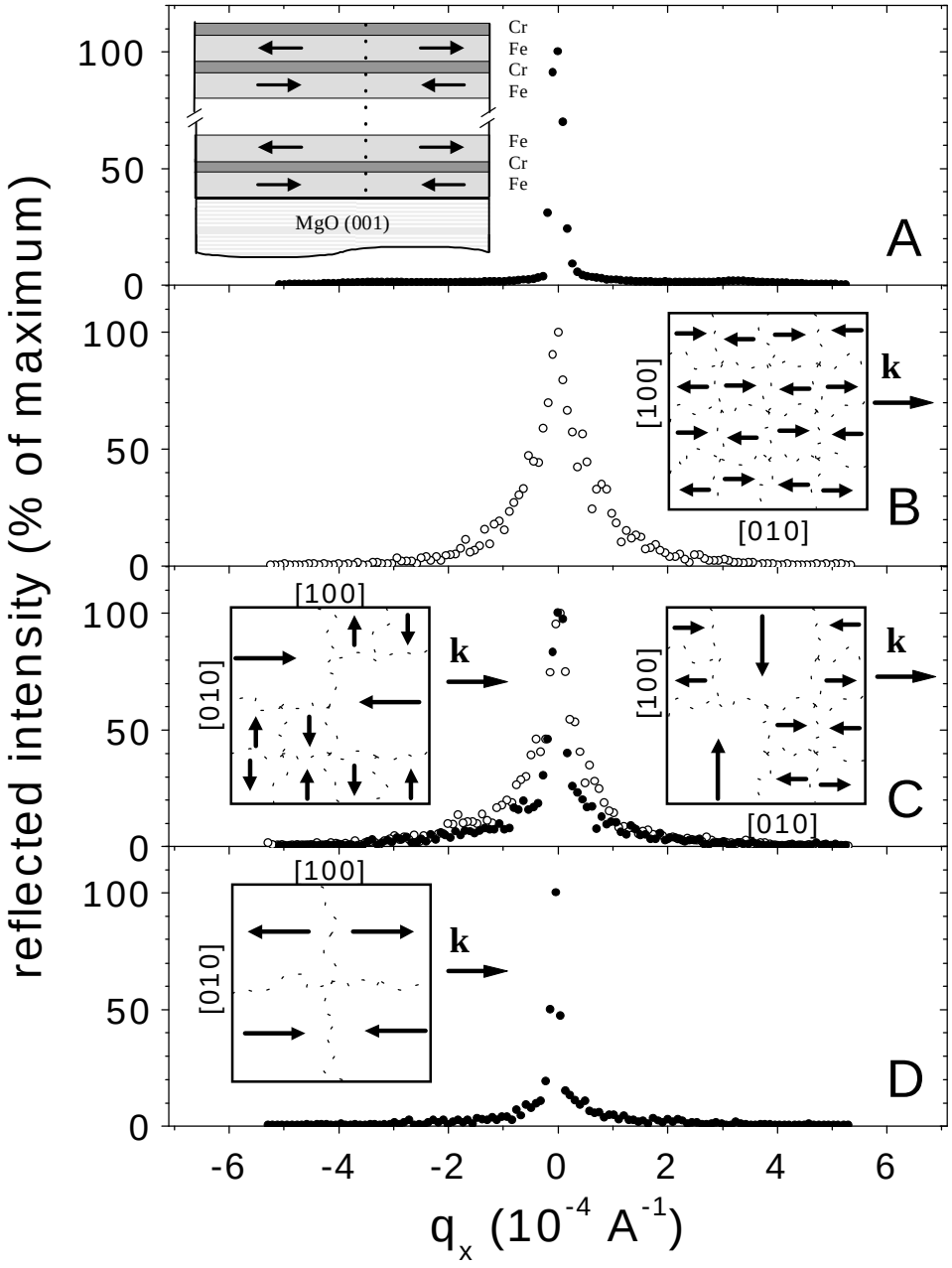

Fig. 3. *Off-specular prompt x-ray and SMR ω-scans. Reflected intensity vs. scattering vector component* $q_x = 2k\Theta(\omega - \Theta)$ *of a MgO(001)/[*^{57}*Fe(26Å)/Cr(13Å)]*$_{20}$ *multilayer at the AF Bragg-reflection (*$\Theta = 0.4°$*) measured in zero external magnetic field: A) prompt reflectivity, not being dependent on magnetic field prehistory, B–D) delayed reflectivity, B) following magnetic saturation, C) following exposure to 13 mT parallel to the magnetizations (open circles: non-flipped domains, full circles: flipped domains), D) following exposure to a field of 35 mT. Inset A is a schematic side view of the chemical and magnetic structure of the sample near to a domain wall (dotted line). Insets B–D are schematic top views of the orientation of the crystallographic axes and of the top-layer magnetizations (short and long arrows represent small and large domains, respectively) relative to the photon wave vector k. [11]*

First the sample was saturated in plane in one of the easy directions then the external field was decreased to zero. At this stage the sample was turned in plane by 90° and TISMR scans were recorded as a function of increasing external magnetic fields. Fig. 2 shows the normalised intensity of the AF peak as a function of the increasing magnetic field. The appearance of the 1/2 and 3/2 order AF reflections around 13.2 mT is a direct evidence of the 90° rotation of the Fe layer magnetisations, i.e., of the bulk-spin-flop process. Due to the fourfold symmetry of the anisotropy, this state is preserved after the magnetic field is removed.

5. Antiferromagnetic domains in multilayers

Domain structure of AF-coupled multilayers is an issue of both theoretical and technological importance. Domain-size-dependent resistance noise, for example, may be as large as to limit GMR-sensor applications [29]. It is extremely difficult to visualise *in-plane AF domains* in a multilayer of few nm thickness. In fact, Kerr-microscopy has been performed so far only on thick trilayers [30,31].

Therefore indirect methods like resistance noise [29] and magnetoresistance [32] measurements, off-specular non-polarised [33] and polarised neutron reflectometry [20,34] and, recently, soft-x-ray resonant magnetic diffuse scattering [5] have been used to estimate the AF-domain-size distribution in metallic multilayers.

Off-specular SMR is, as shown in Section 2, also suitable to investigate the in-plane correlation length of AF domains in coupled multilayers. Off-specular SMR scans of a MgO(001)/[^{57}Fe(26Å)/Cr(13Å)]$_{20}$ multilayer at the AF reflection of $\Theta = 0.4$ deg in two different states, depending on the magnetic prehistory [11] are shown in Fig. 3. The domain size or, more precisely, the magnetisation correlation length ξ can be evaluated from the width of the off-specular ω-scan using Equation (2). The broad line in scan B corresponds to AF microdomains of correlation length $\xi \approx 2.6$ μm. In contrast to this, scan D is the sum of a broad diffuse shoulder (22 % of the total area) and a narrow specular line (78 %). In this state 22 % of the multilayer consists of microdomains ($\xi \approx 2.6$ μm) while the majority of the multilayer contains large domains. Due to the finite aperture of the detector, only a lower limit of the correlation length ($\xi > 16.5$ μm) can be deduced from the width of the specular peak. The explosion-like transition from the primary small-domain state to the secondary state of majority large domains is induced by a bulk-spin-flop transition, which takes place in the sample when a magnetic field of 13 mT is applied along the easy axis in which the layer magnetisations actually lay [11].

The domain coarsening can be monitored by off-specular PNR, without rotating the sample. Prior to the PNR experiment, the sample was magnetically saturated and mounted in remanence with magnetisation parallel/antiparallel to the incident neutron polarisation. PNR maps taken in increasing external field are shown in Fig. 4. Left and right columns in Fig. 4 represent non-spin-flip and spin-flip reflectivities (here R^{--} and R^{-+}), corresponding to magnetization components parallel/antiparallel and perpendicular to the neutron spin, respectively. In a field below the bulk-spin-flop transition (Fig. 4A), the AF reflection appears only in the non-spin-flip channels and consists of a broad diffuse sheet. In contrast, in Fig. 4C, in a field above the transition, the AF reflection is only observed in the spin-flip channels. While the non-spin-flip channels consist only of off-specular diffuse sheets, the spin-flip channels show mainly specular scattering. Midway the transition (Fig. 4B), the AF reflection shows up in both channels, in full accordance with the SMR results.

The formation of the microdomains can be qualitatively understood by the following consideration. The coupling strength between the ferromagnetic layers is subject to an unavoidable lateral distribution of correlation length ξ. Gradually decreasing the external magnetic field from saturation, first the strongest-coupled regions have the freedom to 'decide' whether their odd and even layers start rotating clockwise and anticlockwise, respectively, or *vice versa*. Upon further decreasing the field, the layer magnetisation direction of the neighbouring regions becomes unstable. The minute AF domain-wall

energy becomes decisive in this state and the neighbouring regions nucleate on the already rotated regions, so that the sense of rotation of the individual layers is preserved. The nucleation goes on until the whole multilayer becomes unsaturated and will consist of two kinds of AF patch-like domains [30] differing in the sense of rotation of their odd and even layers [35–37].

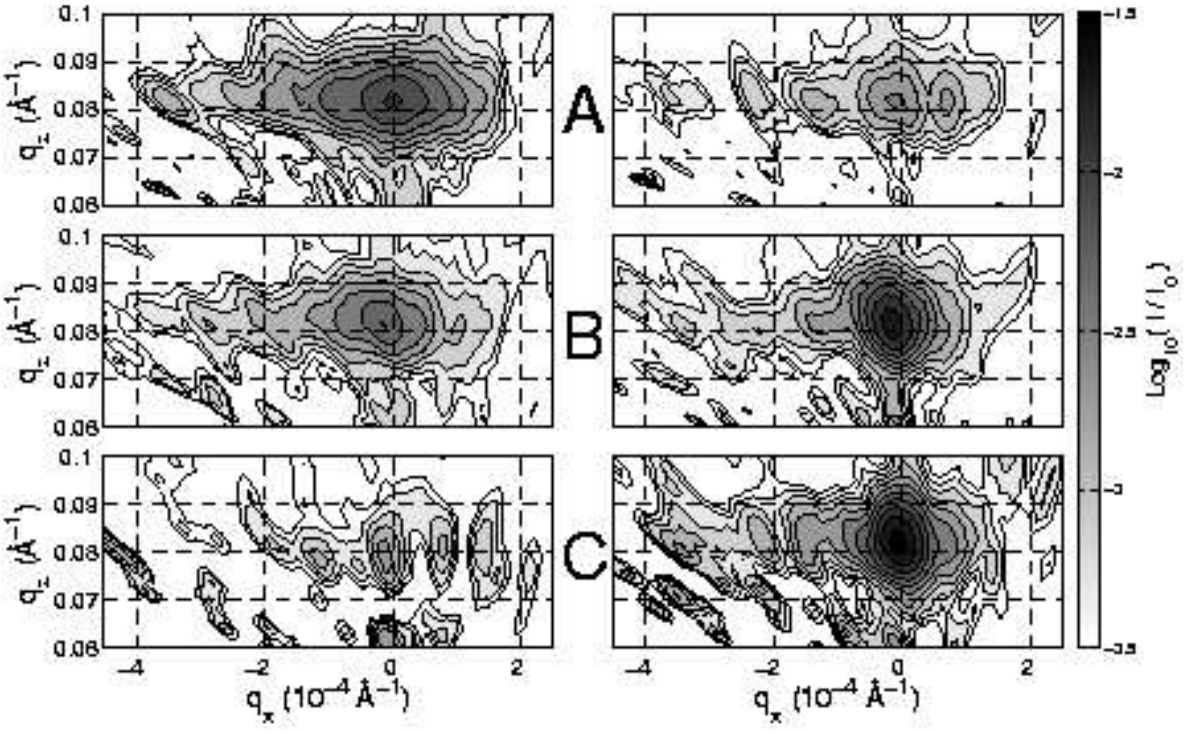

Fig. 4. *Normalised neutron reflectivity maps. Polarised neutron intensity scattered specularly and off-specularly by a MgO(001)/[^{57}Fe(26Å)/Cr(13Å)]$_{20}$ multilayer in a magnetic field of A) 7 mT, B) 14.2 mT and C) 35 mT in R^{--} (left side) and in R^{-+} (right side) channels as a function of the scattering vector components q_x and q_z. [11]*

On further decreasing the field, the specific domain-wall energy increases with increasing domain-wall angle. Therefore the domains are spontaneously increasing in order to decrease the domain-wall energy. The spontaneous growth is limited by the coercivity (Barkhausen effect). We have recently shown [38] how this 'ripening' process can be followed by off-specular SMR and PNR.

6. Summary and acknowledgements

SMR has become an efficient tool in studying magnetic structure of multilayers. AF coupling results in pure nuclear superstructure reflections in time integral SMR experiments. The intensity of the AF reflection is a measure of the in-plane orientation of the layer magnetisation. Time-differential specular SMR experiments can be used to determine both in-plane and out-of-plane layer magnetisation components. Bulk-spin-flop transition results in a sudden change of the AF peak intensity. Off-specular (diffuse) SMR scans show broad shoulders for AF microdomains and sharp specular lines for large domains (a few tens of μm or more).

The authors acknowledge the European Synchrotron Radiation Facility Grenoble and the Joint Institute for Nuclear Research Dubna for provision of synchrotron radiation and pulsed neutron facilities,

respectively. They are very much grateful to the members of IKS of the University of KU Leuven, the nuclear resonance groups of the ESRF and the University of Hamburg and the polarised neutron reflectometry group of JINR for many stimulating discussions. Support by the project No. T 029409 of the Hungarian Scientific Research Fund (OTKA) and by the Hungarian Academy of Sciences, Contract No. 2000-103 2,3 is gratefully acknowledged.

7. References

1. H. Kiessig, *Ann. Phys. (Leipzig)* 10, 715, (1931)
2. E. Fermi and W. Zinn, *Phys. Rev.* 70, 103, (1946)
3. M. Born and E. Wolf, *Principles of Optics*, p. 51, Pergamon Press, Oxford (1970)
4. M. Lax, *Rev. Mod. Phys.* 23, 287, (1951)
5. T.P.A. Hase, I. Pape, B.K. Tanner, H. Dürr, E. Dudzik, G. van der Laan, C.H. Marrows and B.J. Hickey, *Phys. Rev. B* 61, R3792, (2000)
6. S.M. Irkaev, M.A. Andreeva, V.G. Semenov, G.N. Belozerskii and O.V. Grishin, *Nucl. Instrum. Methods B* 74, 545, (1993)
7. E. Gerdau, R. Rüffer, H. Winkler, W. Tolksdorf, C.P. Klages and J.P. Hannon, *Phys. Rev. Lett.* 54, 835, (1985)
8. A.Q.R. Baron, J. Arthur, S.L. Ruby, A.I. Chumakov, G.V. Smirnov and G.S. Brown, *Phys. Rev. B* 50, 10354, (1994)
9. L. Deák, L. Bottyán and D.L. Nagy, *Hyp. Int.* 92, 1083, (1994)
10. T.L. Toellner, W. Sturhahn, R. Röhlsberger, E.E. Alp, C.H. Sowers and E.E. Fullerton, *Phys. Rev. Lett.* 74, 3475, (1995)
11. D.L. Nagy, L. Bottyán, B. Croonenborghs, L. Deák, B. Degroote, J. Dekoster, H.J. Lauter, V. Lauter-Pasyuk, O. Leupold, M. Major, J. Meersschaut, O. Nikonov, A. Petrenko, R. Rüffer, H. Spiering and E. Szilágyi, *Phys. Rev. Lett.* 88, 157202 (2002)
12. D.L. Nagy, L. Bottyán, L. Deák, J. Dekoster, G. Langouche, V.G. Semenov, H. Spiering and E. Szilágyi, in: *Mössbauer Spectroscopy in Materials Science*, M. Miglierini and D. Petridis, Eds., p. 323, Kluwer Academic Publishers (1999)
13. R. Röhlsberger, Hyp. Int. 123/124, 301, (1999)
14. A.I. Chumakov, L. Niesen, D.L. Nagy and E.E. Alp, Hyp. Int. 123/124, 427, (1999)
15. D.L. Nagy, L. Bottyán, L. Deák, E. Szilágyi, H. Spiering, J. Dekoster and G. Langouche, *Hyp. Int.* 126, 353, (2000)
16. D.L. Nagy, L. Bottyán, L. Deák and M. Major, *Acta Phys. Polonica A* 100, 669, (2001)
17. D.L. Nagy, L. Bottyán, L. Deák, B. Degroote, J. Dekoster, O. Leupold, M. Major, J. Meersschaut, R. Rüffer, E. Szilágyi, A. Vantomme, *Hyp. Int.* 141/142, 459, (2002)
18. D.L. Nagy, L. Bottyán, L. Deák, B. Degroote, O. Leupold, M. Major, J. Meersschaut, R. Rüffer, E. Szilágyi, J. Swerts, K. Temst and A. Vantomme, *Phys. Stat. Sol. (a)* 189, 591, (2002).
19. L. Deák, L. Bottyán, D.L. Nagy and H. Spiering, *Physica B* 297, 113, (2001)
20. C.F. Majkrzak, *Physica B* 156-157, 619 (1989)
21. G.P. Felcher, *Physica B* 192, 137, (1993)
22. L. Bottyán, J. Dekoster, L. Deák, A.Q.R. Baron, S. Degroote, R. Moons, D.L. Nagy and G. Langouche, *Hyp. Int.* 113, 295, (1998)
23. A.L. Dantas and A.S. Carriço, *Phys. Rev. B* 59, 1223, (1999)

24. R.W. Wang, D.L. Mills, E.E. Fullerton, J.E. Mattson and S.D. Bader, *Phys. Rev. Lett.* 72, 920, (1994)

25. N.S. Almeida and D.L. Mills, *Phys. Rev. B* 52, 13504, (1995)

26. K. Temst, E. Kunnen, V.V. Moshchalkov, H. Maletta, H. Fritzsche and Y. Bruynseraede, *Physica B* 276–278, 684, (2000)

27. L. Bottyán, L. Deák, J. Dekoster, E. Kunnen, G. Langouche, J. Meersschaut, M. Major, D.L. Nagy, H.D. Rüter, E. Szilágyi and K. Temst, *J. Magn. Magn. Mater*. 240, 514 (2002)

28. L. Bottyán, J. Dekoster, L. Deák, B. Degroote, E. Kunnen, C. L'abbé, G. Langouche, O. Leupold, M. Major, J. Meersschaut, D.L. Nagy and R. Rüffer, in: in: *ESRF Highlights 1999*, p. 62, European Synchrotron Radiation Facility, Grenoble (2000)

29. H.T. Hardner, M.B. Weissmann and S.S.P. Parkin, *Appl. Phys. Lett.* 67, 1938, (1995)

30. M. Rührig, R. Schäfer, A. Hubert, R. Mosler, J.A. Wolf and S. Demokritov, P. Grünberg, *Phys. Stat. Sol. A* 125, 635, (1991)

31. R. Schäfer, *J. Magn. Magn. Mater.* 148, 226, (1995)

32. N. Persat, H. A. M. van den Berg and K. Cherifi-Khodjaoui, *J. Appl. Phys.* 81, 4748, (1997)

33. S. Langridge, J. Schmalian, C.H. Marrows, D.T. Dekadjevi and B.J. Hickey, *Phys. Rev. Lett.* 85, 4964, (2000)

34. V. Lauter-Pasyuk, H.J. Lauter, B. Toperverg, O. Nikonov, E. Kravtsov, M.A. Milyaev, L. Romashev and V. Ustinov, *Physica B* 283, 194, (2000)

35. N. Persat, H.A.M. van den Berg and K. Cherifi-Khodjaoui, *J. Appl. Phys.* 81, 4748, (1997)

36. M. Major, L. Bottyán, D.L. Nagy, *J. Magn. Magn. Mater*. 240, 469 (2002)

37. M. Major, L. Bottyán, D.L. Nagy, Phys. Stat. Sol. (a)189, 995, (2002)

38. M. Major, L. Bottyán, B. Croonenborghs, L. Deák, J. Dekoster, O. Leupold, D.L. Nagy, Yu. Nikitenko, A. Petrenko, V.V. Proglyado, R. Rüffer, E. Szilágyi, to be published